Available online at www.sciencedirect.com

SCIENCE DIRECT®

Earth and Planetary Science Letters 236 (2005) 691–704

EPSL

www.elsevier.com/locate/epsl

A plate tectonic mechanism for methane hydrate release along subduction zones

A. Hope Jahren [a,*], Clinton P. Conrad [a], Nan Crystal Arens [c], German Mora [d], Carolina Lithgow-Bertelloni [b]

[a] *Department of Earth and Planetary Sciences, Johns Hopkins University, Baltimore, MD 21218, USA*
[b] *Department of Geological Sciences, University of Michigan, Ann Arbor, MI 48109, USA*
[c] *Department of Geosciences, Hobart and William Smith Colleges, Geneva, NY 14456, USA*
[d] *Department of Earth and Atmospheric Sciences, Iowa State University, Ames, IA 50011, USA*

Received 24 January 2005; received in revised form 26 May 2005; accepted 9 June 2005

Editor: E. Boyle

Abstract

Negative carbon isotope excursions from a new record of terrestrial organic carbon ($\delta^{13}C_{org} = -2.3‰$) and from marine carbonate ($\delta^{13}C_{carb} = -0.8‰$) were used to calculate a methane hydrate release of 1137 Gt of carbon over ~1 Myr during the early Aptian (Early Cretaceous). We show how the coincident and sudden near-cessation of subduction along the northern boundaries of the Farallon plate resulted in uplift along the continental margin by up to 4.0 km, which may have triggered the release. We conservatively estimated the amount of methane hydrate carbon likely to have been destabilized during the uplift and found it to be within 20% of the amount of carbon implied by the isotopic records within the same ~1 Myr time frame. Linking subduction-triggered destabilization with isotopic evidence for methane release reveals a plate tectonic mechanism for the incorporation of methane hydrate release into long-term carbon cycling.
© 2005 Elsevier B.V. All rights reserved.

Keywords: methane hydrate; Aptian; seismic coupling; carbon isotope excursion; terrestrial organic matter

1. Introduction

Methane hydrates constitute a large global carbon reservoir that is vulnerable to destabilization via ocean-floor disruption. Such destabilization has important implications for the global cycles of both carbon and methane, especially with respect to atmospheric chemistry and potential climate warming. Integration of methane hydrate reservoir dynamics into

* Corresponding author. Tel.: +1 410 516 7134; fax: +1 410 516 7933.
E-mail addresses: jahren@jhu.edu (A.H. Jahren), cpconrad@umich.edu (C.P. Conrad), arens@hws.edu (N.C. Arens), gmora@iastate.edu (G. Mora), crlb@umich.edu (C. Lithgow-Bertelloni).

0012-821X/$ - see front matter © 2005 Elsevier B.V. All rights reserved.
doi:10.1016/j.epsl.2005.06.009

a long-term understanding of the carbon cycle [1] requires recognition of multiple methane-release events. In all of Earth's history, only one methane hydrate release is generally uncontested: ~2500 Gt (10^{15} g) of carbon at the PETM (Paleocene/Eocene thermal maximum; ~55 Ma; [2]). Methane hydrate dissociation has been tentatively proposed at the Permian–Triassic boundary (~248 Ma; [3]), the Early Jurassic (~185 Ma; [4]), the Late Jurassic (~155 Ma; [5]), the Early Cretaceous (~117 Ma; [6]) and during the Neoproterozoic (~1000–542 Ma; [7]). Moreover, sudden deep-ocean warming (the mechanism for the PETM release [8]) may be stochastic and difficult to predict throughout Earth's history. Here we show how major tectonic events led to a methane hydrate release in the early Aptian (Early Cretaceous), as evidenced by a new high-resolution terrestrial $\delta^{13}C$ (carbon stable isotope) record. We suggest that plate tectonics, a fundamental Earth process, may control methane hydrate reservoir disruption over long timescales via deformation of the continental margins.

2. A new record of Aptian terrestrial δ^{13}_{Corg}

We sought to confirm the negative $\delta^{13}C$ excursion seen in stratigraphically limited organic samples from

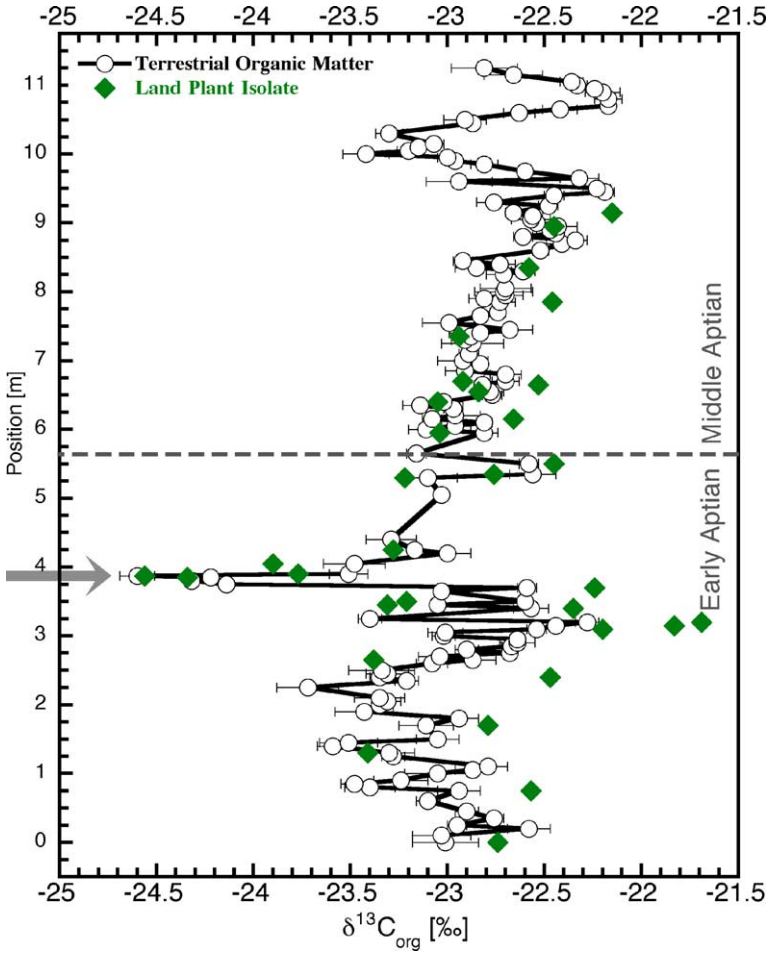

Fig. 1. Stratigraphic presentation of $\delta^{13}C_{org}$ values for bulk organics and cuticle isolates from the United Clay Mine; error bars reflect the standard deviation seen in three replicate analyses. The dashed gray line represents the boundary between the early and middle Aptian approximated using palynological data and sedimentation rates. The isotopic shift is highlighted by a gray arrow at ~4 m.

near-shore environments [6,9–11] with high-resolution $\delta^{13}C$ analyses of wholly terrestrial sediments, in order to establish the early Aptian terrestrial C-isotope excursion as a global event. We sampled the Arundel Clay Formation of the Potomac Group within Maryland: 11 m of exposed section were sampled at 5–10 cm increments in order to capture variations in lamination and organic matter content. Plant cuticle was isolated from sediment sub-samples in order to verify terrestrial origin; both bulk organic matter and cuticle were analyzed for $\delta^{13}C$ value (see Appendix A). Pollen and spores from three widely spaced samples indicated that the United Clay Mine section is early to middle Aptian in age (see Appendix A), in keeping with previous studies [12]. The estimated duration of the early and middle Aptian is ~6 Myr; a conservative analysis of the Arundel Formation (~11 m in this locality) suggests a sedimentation rate of ~1.8 m/Myr. Using this estimate, the negative excursion near 4 m (Fig. 1) took place in less than 1 Myr: $\delta^{13}C_{org} = -2.3‰$ for bulk samples; $-2.9‰$ for cuticle isolates. This is similar to trends in $\delta^{13}C_{org}$ values of early Aptian terrestrial materials from Europe [9,11] and South America [6], confirming the early Aptian terrestrial C-isotope excursion as a global signal. The value of the Arundel Clay excursion is less than the

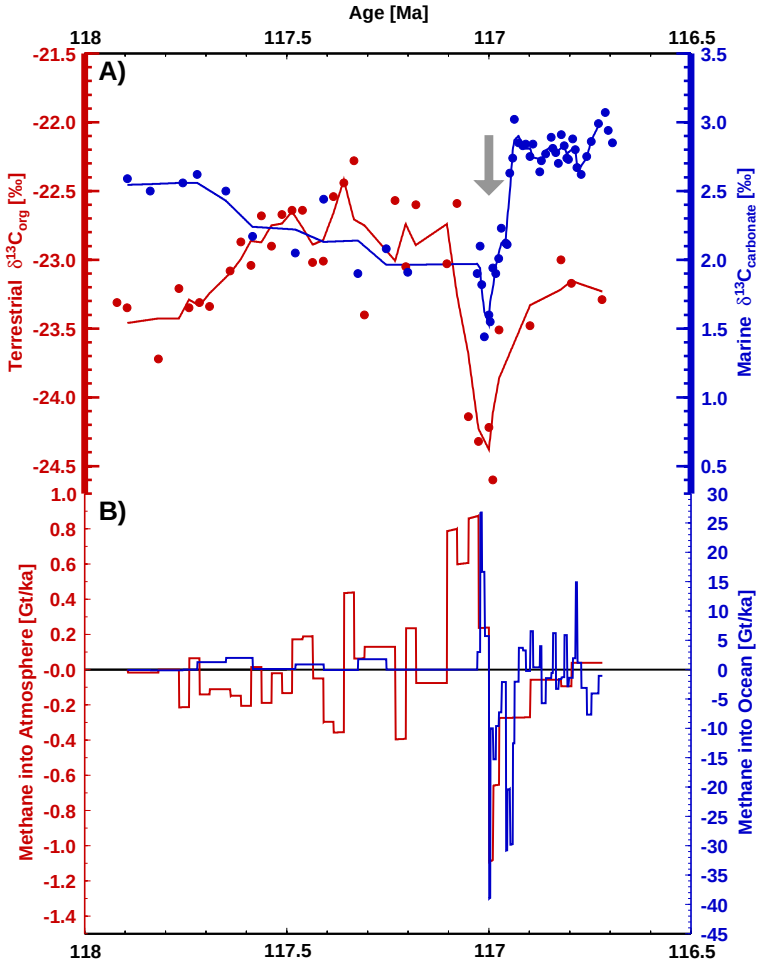

Fig. 2. The terrestrial isotopic shift in Fig. 1 (at 4 m) presented relative to the marine $\delta^{13}C_{carbonate}$ values of Menegatti et al. [13], each illustrated with a three-point running mean (A). The most negative point in each record (both independently dated as early Aptian) were aligned (gray arrow), and data preceding and succeeding were positioned according to sedimentation rates (terrestrial) and nannofossil zones (marine). The early Aptian methane release in terms of Gt of carbon (B) was calculated in 1000-yr increments using Eqs. (2) and (3) within the main text.

value of the excursion we observed in Colombian sediments ($\delta^{13}C_{org} = -4.9‰$ [6]) and larger than the early Aptian excursion found in marine carbonates (e.g., $\delta^{13}C_{carb} = -0.8‰$ [13] and Fig. 2A). We submit that these differences arise from the great differences in temporal sampling density between the studies. Because the isotopic measurements made during this study represent greatly enhanced sampling density within a singly terrestrial paleoenvironment, well-preserved by decomposition-resistant clay [14], we contend that the dataset presented here constitutes a more realistic record of global change than previous scenarios based on fewer data points from Aptian terrestrial sediments (e.g., [6,15]).

3. Carbon mass balance from Aptian isotopic records

Changes through time in the $\delta^{13}C_{org}$ value of accumulated terrestrial plant material across substrates that do not differ with respect to carbon content, species composition and alteration index, and which give no indication of changing environmental stress conditions, are best interpreted as a change in the $\delta^{13}C$ value of atmospheric CO_2—the raw material of photosynthesis [16]. We have shown elsewhere that published values of $\delta^{13}C_{org}$ in plant tissues are well-correlated with the $\delta^{13}C$ value of the CO_2 under which the plants grew ($r^2 = 0.91$) and poorly correlated with the pCO_2 level of the environment ($r^2 = 0.002$) [16]. The evaluation of 519 $\delta^{13}C_{org}$ measurements made on 176 C3 (Rubisco-only) vascular land plant species across a wide range of ecophysiological stresses, atmospheric pCO_2 and $\delta^{13}CO_2$ yielded an average isotopic offset ($_{plant-atmosphere}$) $= -18.7‰$ [16] which agreed well with classical estimates of whole-ecosystem carbon isotope fractionation [17]. Because of large C-isotopic variability among individuals and species, inference of changing atmospheric $\delta^{13}CO_2$ value from the $\delta^{13}C_{org}$ value of fossilized terrestrial plant material must be made using a substrate that concentrates the tissue contribution of many individuals from many genera: terrestrial sedimentary organic matter is ideally suited for this application because sedimentary organic matter commonly averages across many different taxonomic groups, providing an integrative measure of plant $\delta^{13}C_{org}$.

The change in early Aptian atmospheric $\delta^{13}CO_2$ value implied by the negative C-isotope excursion measured in the Arundel Clay, taken with Cretaceous CO_2 levels (4× modern ≈ 2400 Gt of C [18]), can be used to determine the source of the carbon isotope perturbation. A negative excursion in atmospheric $\delta^{13}CO_2$ can be produced by an addition of ^{13}C-depleted CO_2 emitted by volcanism ($\delta^{13}CO_2 \approx -8‰$ [19]), from the oxidation of terrestrial biomass ($\delta^{13}CO_2 \approx -25‰$ [20]), or from the oxidation of CH_4 released from methane hydrates ($\delta^{13}CH_4 \approx -60‰$ [21]). Given the above, a simple source-mixing analysis [6] can be used to estimate the mass of carbon (n) required from each of the potential sources mentioned above in order to drive the negative atmospheric excursion:

$$2400\ \text{Gt C}^*\left(\delta^{13}C_{\text{atmosphere}}\ \text{late Barremian}\right) + n\ \text{Gt C}^*\left(\delta^{13}C_{\text{emission}}\right) = 2400 + n\ \text{Gt C}\left(\delta^{13}C_{\text{atmosphere}}\ \text{early Aptian}\right)$$

This simplistic calculation treats the excursion as an instantaneous event (and is therefore an underestimation of the amount of ^{13}C-depleted CO_2 required to affect an atmosphere progressively equilibrating with the ocean). Nonetheless, it identifies methane hydrates as the most likely source of the early Aptian negative $\delta^{13}C$ excursion. The total decrease in atmospheric $\delta^{13}CO_2$ value implied by the excursion in the $\delta^{13}C_{org}$ value of Arundel Clay cuticle (Fig. 1) would require the liberation of 3314 Gt of C from volcanic sources—an increase in atmospheric CO_2 levels from 4× to 9.5× modern in less than 500 kyr: this is an unrealistically large amount, despite the concurrent emplacement of the Ontong Java plateau [22]. We also reject a terrestrial source for this excursion since it requires the combustion of 364 Gt of C, an amount equal to 65% of today's standing biomass [23]; such a massive disruption in Aptian ecosystems has not been seen in paleobotanical records [24]. In contrast, an instantaneous negative excursion can be explained by the liberation and subsequent oxidation of only 129 Gt of C from methane hydrates, which is less than 2% of the CH_4 contained in modern continental margins [25].

Examination of the Arundel Clay $\delta^{13}C$ record in concert with the marine $\delta^{13}C$ record in 1000-yr time intervals sheds light on the methane release proposed

above. A correlated negative excursion in terrestrial $\delta^{13}C_{org}$ and marine $\delta^{13}C_{carb}$ and $\delta^{13}C_{org}$ measurements has been documented from the early Aptian [6,11]. Close examination of Arundel Clay early Aptian $\delta^{13}C_{org}$ values in tangent with the uniquely comprehensive and high-resolution marine $\delta^{13}C_{carb}$ composite record of Menegatti et al. ([13] and Fig. 2A) allows determination of the mass of methane required to simultaneously drive the negative excursions observed in both terrestrial and marine carbon reservoirs. Given M as the mass of carbon [Gt=10^{15} g], the dynamics of the early Aptian carbon release can be envisioned as the following:

$$M_{\text{released}} = M_{\text{into atmos}} + M_{\text{into ocean}} \quad (1)$$

Isotopic mass balance allows for estimation of the amount of carbon released into the atmosphere as methane to cause the negative excursion presented in Fig. 2A:

$$M_{\text{into atmos}} = M_{\text{atmos, } t_0} \times \left(\frac{\delta^{13}C_{\text{atmos, } t=t_0+1000} - \delta^{13}C_{\text{atmos, } t_0}}{\delta^{13}C_{\text{methane}} - \delta^{13}C_{\text{atmos, } t=t_0+1000}} \right) \quad (2)$$

where M_{atmos,t_0}=2400 Gt [26], $\delta^{13}C_{atmos}$ is specified according to the isotopic offset described above and $\delta^{13}C$ methane=−60‰ [21]. Likewise, the amount of carbon as methane released into the ocean can be estimated according to the following:

$$M_{\text{into ocean}} = M_{\text{DIC, } t_0} \times \left(\frac{\delta^{13}C_{\text{DIC, } t=t_0+1000} - \delta^{13}C_{\text{DIC, } t_0}}{\delta^{13}C_{\text{DIC}\leftrightarrow\text{methane}} - \delta^{13}C_{\text{DIC, } t=t_0+1000}} \right) \quad (3)$$

where $\delta^{13}C_{DIC}$ is calculated from $\delta^{13}C_{carb}$ using $\alpha^{CaCO_3}_{HCO_3^-}$=1.002 and $\delta^{13}C_{DIC\leftrightarrow methane}$ is calculated from $\delta^{13}C_{methane}$ using $\alpha^{CO_2}_{HCO_3^-}$=0.992 [27], given that the oxidation of CH_4 to CO_2 proceeds without fractionation of $^{13}C/^{12}C$ [28]; modern M_{DIC,t_0}=36,600 Gt [29] and has not fluctuated greatly during the Phanerozoic [30]. Our estimates can be taken to represent the minimum injection of methane into the carbon cycle (particularly that of the atmosphere), since neither Eq. (2) nor Eq. (3) contains a term describing the exit of released carbon from the system prior to influencing the carbon isotope record; the magnitude of such an exodus over long timescales is poorly constrained [31,32]. This model envisions that one portion of any methane release was partially oxidized within the ocean, thus depleting the dissolved inorganic carbon (DIC) pool and then the carbonate ($CaCO_3$) pool in ^{13}C. We also include the oxidation of the remaining portion of the methane release in the atmosphere, given the probable transport of gaseous CH_4 through the water column and into the atmosphere [33]. Under this vision, the portion of methane oxidized in the atmosphere resulted in ^{13}C-depleted CO_2 which then became the raw material of photosynthesis.

Mass balance calculations have been performed in 1000-yr increments (the timescale of isotopic equilibrium between the atmosphere and the deep ocean). The mass of methane release thus calculated incrementally from three-point running averages (Fig. 2A) of carbon isotope data=1137 Gt over approximately 1 Myr (Fig. 2B); This value represents 11% of the global reservoir of carbon currently stored in methane hydrates [25]. Nine percent of this total represents carbon released into the atmosphere, while the majority constitutes carbon as CH_4 oxidized to CO_2 and subsequently equilibrated into the active DIC pool. It is notable that the mass ratio of atmospheric to oceanic methane release (1:8) is comparable to the mass ratio of carbon in the atmosphere to that in the surface and intermediate ocean (1:6.5) [34]. Note that if one instead prefers the interpretation that atmospheric $\delta^{13}CO_2$ is entirely set, and thus progressively changed, only by equilibration with oceanic $\delta^{13}C$ values, the resulting estimate of carbon from CH_4 release (1057 Gt) is not significantly different from that above. Our analysis suggests that the majority of the methane was released within a few hundred thousand years at the rate of ~1.0 Gt CH_4/kyr. The net movement of carbon within the system approaches zero over ~1 Myr, indicating that carbon with composition $\delta^{13}C$=−60‰ has been removed from both reservoirs, particularly from the oceanic pool (Fig. 2B).

The above calculations assume no ^{13}C-isotope depletion or enrichment as CH_4 moves from solid to either dissolved or free-gaseous phase, either within the ocean or within the atmosphere (e.g., page 175 of [1]); in addition, workers have suggested that abiotic oxidation of CH_4 imparts little or no change in $\delta^{13}C$

value [28]. However, bacterial oxidation of CH_4 to CO_2 has long been known to result in the enrichment of ^{12}C (e.g., [35]). For example, the carbon kinetic isotope effect imparted by aerobic bacteria during the oxidation of CH_4 ($\alpha_{C_{ox}}^{CO_4}$) has been measured to range from 1.003 to 1.039 within laboratory cultures and terrestrial soil environments (reviewed in [36]). Such large-scale fractionation would clearly affect the values of $\delta^{13}C_{DIC}$ involved in the calculation of Eq. (3) above. However, integration of this effect into any oceanic mass balance (e.g., Eqs. (1)–(3)) would require: (1) knowledge of the relative amount of CH_4 that is oxidized microbially vs. abiotically during and after a marine methane release of methane hydrates; (2) the extent to which the fractionation factors above, gained within terrestrial systems, may be applied to oceanic sedimentary environments; (3) specific determination and use of one value of ($\alpha_{C_{ox}}^{CO_4}$) from within the wide range of enrichments that have been reported (e.g., [36]). At present, each of these issues remains contentious; however they should be kept in mind as a potential enrichment of ^{13}C, prior to its full incorporation into the DIC pool. Similarly, there exist questions of the potentially large isotopic fractionation of carbon (e.g., [37]) within the atmosphere prior to incorporation into the photosynthetic biota. This fractionation would result from reactions between OH and CH_4 within the atmosphere, which comprise ~43% of the modern atmospheric methane sink [38]. However, an important obstacle in the application of these values to Eqs. (1)–(3) (above) is the belief that, over long timescales, a continuous release of methane would likely exceed the atmosphere's capacity for oxidation [39]. Our mass-balance model may not adequately describe every conceivable fractionation of carbon that might come into play as methane hydrate is released into marine and terrestrial systems; a more complete picture will no doubt emerge given contemporary focus on modern oceanic methane hydrate reservoirs (e.g., [40]).

4. Reconstruction of Aptian tectonic plate motions

An abrupt change in the tectonic setting of the Pacific basin occurred during the early Aptian, as shown by our reconstructions of plate motions (Fig. 3A and B); we propose that this tectonic change carried important consequences for methane hydrates stored in the continental margins. Multiple authors have characterized the mid-Cretaceous as a time of significant tectonic activity. Larson [41] noted a simultaneous increase in the rates of both oceanic plateau production and seafloor spreading in the Pacific Basin during the mid-Cretaceous and proposed that both were generated by a "superplume" rising through the mantle and impinging on the lithosphere. Jahren [42] previously proposed this superplume as a driver of the early Aptian terrestrial carbon isotope excursion using a semi-quantitative description of possible seafloor uplift. Vaughan [43] noted evidence for deformation of plates overriding subduction zones around the Pacific Basin and suggested that a pulse of seafloor spreading could increase rates of subduction and deformation of overriding plates. Evidence for a pulse of mid-Cretaceous rapid seafloor spreading has been disputed (e.g., [44,45]), because marine geochemistry does not support such a pulse, and elevated sea level during this time can be explained by supercontinent breakup instead of rapid seafloor spreading in the Pacific Basin. Detailed tectonic reconstructions of the Pacific Basin [46] indicate that a major reorganization of Pacific plate motions occurred during the early Aptian (Fig. 3A and B). These reconstructions show a general slowing of the Farallon plate, but increased spreading rates for the ridges of the plate's southern boundary. The preferential preservation of seafloor produced by these ridges (as opposed to those farther north, which have been subducted) explains part of the observed pulse of spreading rates during the Aptian. Close inspection of motions for the Farallon plate (Fig. 3)) reveals that during the Barremian and early Aptian (i.e., prior to ~117 Ma), the northwestern portion of the plate moved rapidly in a northerly direction (Fig. 3A). Later in the early Aptian (i.e., after ~117 Ma), Farallon plate motion changed such that the northward motion in the northwestern portion slowed significantly while northward motion of the southeastern portion accelerated (Fig. 3B).

We calculated plate motions and subduction rates for the Early Cretaceous using Engebretson's [46] poles of rotation in a hotspot reference frame and plate boundaries (Fig. 3A and B) taken from Lithgow-Bertelloni and Richards [47]. The Farallon plate (shown in white) is surrounded by (clockwise from the

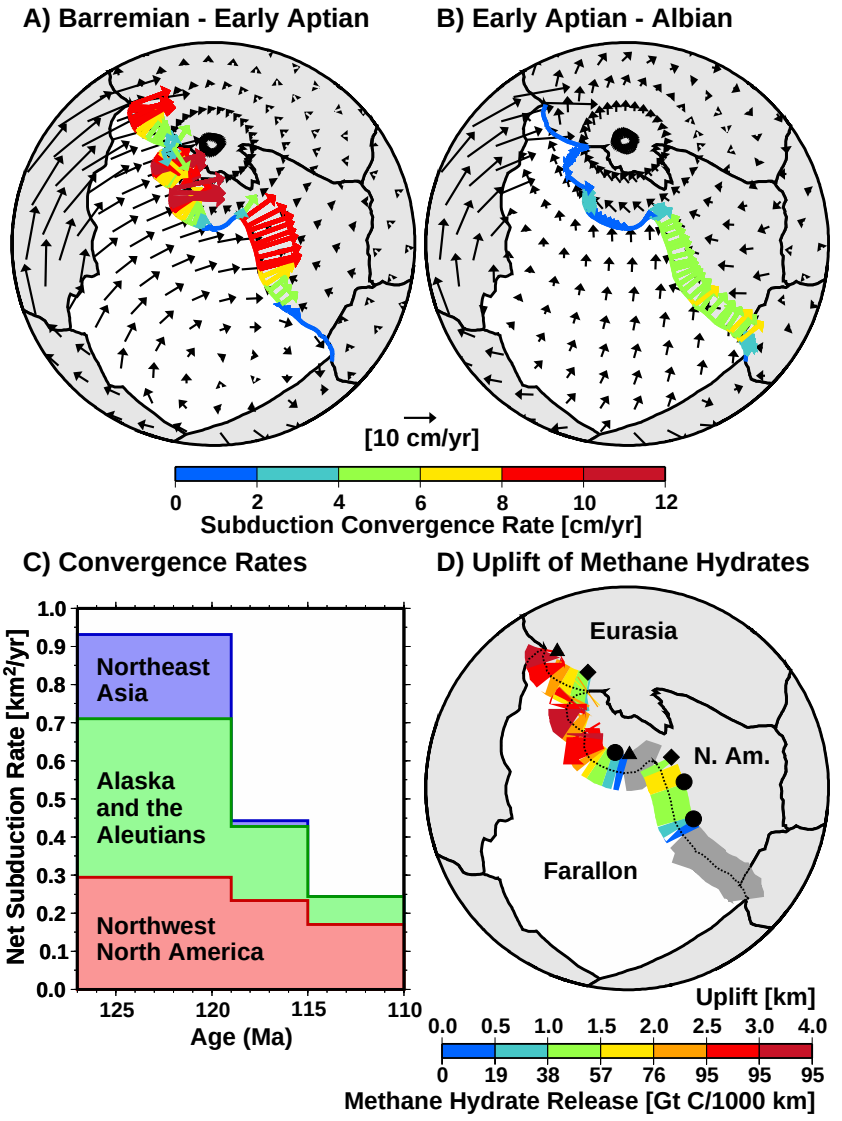

Fig. 3. Plate motion and subduction of the Farallon plate for the time periods prior to 119 Ma (A; Barremian and early Aptian) and after 115 Ma (B; Early Aptian–Albian) [46]. The Farallon plate is shown in white; black arrows show plate velocities and colored arrows show rates of convergence between subducting and overriding plates along the northern boundaries of the Farallon plate. A dramatic decrease in subduction beneath the convergent margins of the Farallon plate is apparent within the early Aptian (C). This decrease resulted from the locking of the boundary between the subducting and overriding plates (Fig. 4). Sudden locking of the plate boundary resulted in horizontal shortening and uplift of the continental margin (D; gray represents zero uplift). Regions of predicted uplift correspond to geological observations of uplift [43] in the early Aptian (D) denoted by ocean-vergent overthusting (●: California, British Columbia, Alaska), amphibolite facies and Sanbagawa metamorphism (▲: Alaska and Japan), and regionally extensive unconformities (◆: Northeast Russia and Northwest Canada).

top) the Eurasian, North American, South American, Phoenix, Pacific, and Izanagi plates. Engebretson et al.'s [46] reconstruction of Farallon plate motion is constrained by the trace of the Mendocino Fracture zone, which records nearly constant relative motion between the Farallon and Pacific plates throughout the Long Normal Superchron (LNS; began at ~120 Ma). A bend in this fracture zone preserved in seafloor

material produced immediately prior to the LNS records a change in plate motion that occurred within a few million years during the early Aptian [48], validating our assertion that these changes are concurrent with the carbon isotope excursions detailed above.

5. Changes in Aptian subduction and resultant uplift

Prior to the early Aptian change in plate motion, the Farallon plate subducted rapidly and continuously beneath northeastern Eurasia (presently Kamchatka, the Kuriles, and Japan), Alaska and the Aleutians, and northwest North America (presently British Columbia through California) (colored arrows within Fig. 3A). In contrast, when plate motion changed (~117 Ma), subduction beneath these convergent margins ceased or slowed, while subduction beneath southwestern North America (presently Central America) accelerated slightly (colored arrows within Fig. 3B). This is demonstrated by rapid decreases in the net subduction rate (Fig. 3C), calculated by summing the product of the convergence rate and segment length for three subduction zones. The decrease in subduction along the northern margin of the Pacific basin coincides with several geological observations of compression and uplift of the continental margin during the early Aptian ([43]; Fig. 3D).

The early Aptian changes in subduction along the Farallon plate's northern boundaries (Fig. 3A and B) necessitate dramatic deformation of the active continental margin, where methane hydrates reside. We consider a scenario where rapid changes in plate motions are driven by changes in friction within subduction zones [49]. Prior to the Aptian, the Farallon plate subducted smoothly and rapidly (Fig. 4A); after the Aptian, subduction ceased or slowed (Fig. 4B). This dramatic slowing of subduction (Fig. 3C) was coincident with extensive compression of the continental margin (Fig. 3D; e.g., [43,50]). Observations of both slowing and compression can be explained by an increase in friction along the interface between the subducting and overriding plates. As this friction increased, the overriding and subducting plates became locked, and convergence inherent to subduction was manifested as compression and deformation of the continental margin ([51]; Fig. 4). This initiated the feedback process described by Conrad et al. [49]. Because slab rheology is stress-dependent, increased mechanical coupling at the convergent zone, and the resultant compressive stresses that are applied to the subducting slab, weakened the slab and caused it to partially detach from the subducting plate. This detachment not only diminished the slab pull force, which slowed the trenchward motion of the subducting plate, but it also allowed the slab to descend more rapidly into the upper mantle. The faster descent induced convergent viscous flow of the upper mantle that pushed subducting and overriding plates together and reinforced compression across the plate boundary. This further increased friction along the plate boundary ([49]; Fig. 4B), creating a feedback that ultimately resulted in the uplift and deformation of the entire northern boundary of the Farallon plate (Fig. 3D), as verified by geological observations [43].

When increased frictional interaction between a subducting and an overriding plate impedes subduction, the convergence associated with subduction will compress the lithosphere surrounding the plate boundary. This type of compression, which is currently observed in mechanically coupled subduction zones such as those in Chile, Alaska, and Kamchatka [51,52], results in thickening of the crustal layer of the overriding plate (Fig. 4). The amount of crustal thickening (Δh) can be estimated by first assuming that the decrease in subduction rate (Δv) observed during the early Aptian (compare colored arrows of Fig. 3A and B) results in shortening of the overriding plate's crustal layer (Fig. 4) during a time interval (Δt) of 1 Myr, as estimated from the duration of the isotopic excursion. If the change in the original convergence rate is accommodated by shortening during this time period, then the amount of shortening will be given by ($\Delta v t$). If this shortening is accommodated over a constant distance W (Fig. 4B) and the original crustal thickness is h, then (assuming pure shear) the total thickening is given by $\Delta h = \Delta v \Delta t / W$. Crust (density = 2.8 g/cm^3) uplifting into water (density = 1.0 g/cm^3) will become isostatically compensated at depth, which will cause only 21.7% of the thickening to manifest itself as surface uplift (assuming mantle density of 3.3 g/cm^3). We assume a crustal thickness equal to today's average of $h = 38$ km [53]; although observed crustal thickness variations include extreme values that differ from this global average by up 2×,

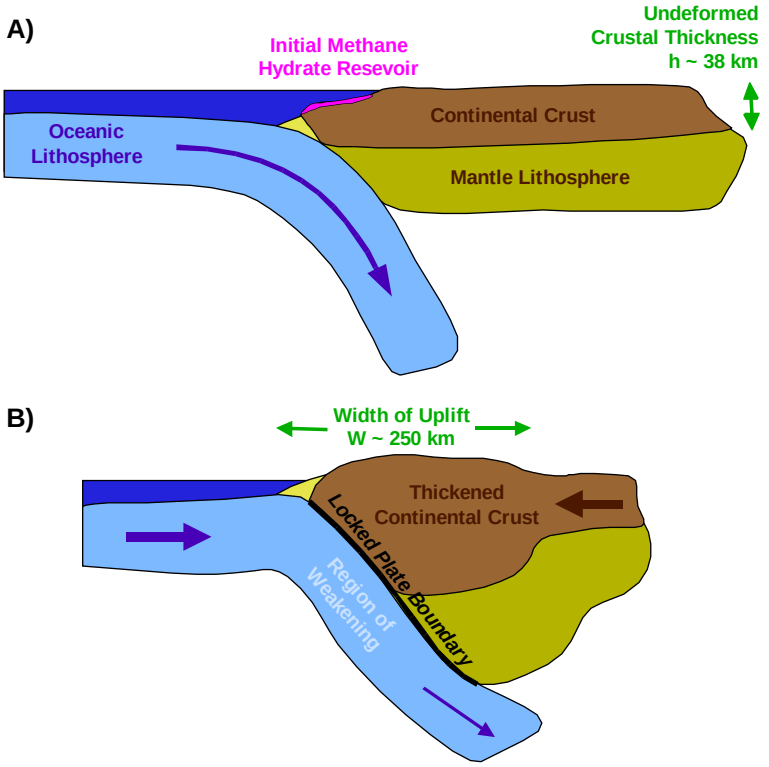

Fig. 4. Graphic illustration of Farallon plate subduction beneath the northern boundaries of the Pacific basin during the early Aptian. Prior to the early Aptian, subduction proceeded efficiently (A); during the early Aptian, increased friction between the subducting Farallon plate and the overriding North American and Eurasian plates caused the boundary between them to become locked (B). Because subduction was impeded, the horizontal motion of the Farallon plate is instead accommodated by shortening and thickening of the overriding plate (B). Crustal thickening occurs above the locked plate boundary and uplifts the continental margin, raising stored methane hydrates out of the stability zone and thus destabilizing them to release methane. In addition, associated stresses exerted on the slab may weaken it, removing slab pull forces [49] and causing additional uplift [62].

such variations are diminished when averaged along the 15,000 km length of subduction treated here. A greater uncertainty is associated with estimates of the shortening width W [km] which we take here to have a constant value of $W=250$ km. This is a conservatively large estimate, given our model of uplift. $W=250$ km is consistent with a coupled fault reaching about 100 km depth (the depth above which arc volcanoes form; [54]) with a ~20° dip. Because most slabs dip more steeply than this [54], narrower zones of uplift are probable, which would increase uplift. In fact, an average dip of only ~30° yields $W=175$ km, which leads to uplift rates that are ~40% greater than for $W=250$ km. If we assume $W=250$ km, then the above model for crustal thickening results in the rates of uplift shown in Fig. 3D.

6. Tectonic destabilization of methane hydrates

The deformation of the subuction zones along the northern boundaries of the Farallon plate created conditions that would destabilize methane hydrates stored along the continental margin of these boundaries. Methane hydrates have likely existed at continental margins throughout Earth's history, making it plausible that methane hydrate formation and destabilization occurred during the early Aptian. Research indicates that temperature and pressure conditions are suitable for methane hydrate formation along continental margins throughout geologic time [55–57] with disputes about the relative size of methane hydrate reservoirs in the past. Most workers have suggested that the past reservoir of methane hydrates was larger than at pres-

ent, due to greater organic carbon burial in past oceans (e.g., [58]). However, a recent model describing the sensitivity of the hydrate reservoir to changing O_2 levels, seawater temperature and organic carbon input predicts very low levels of Cretaceous methane hydrate as compared to today [59]. Given these disputes, we considered a conservative scenario in which an amount of clathrates equal to today's reservoir ($\approx$ 10,000 Gt of C; [25]) is evenly distributed between active and passive margins (a conservative assumption given that much of what is now the Atlantic basin was fused within Gondwanaland during the Aptian). The length of subduction zones affected by the change in Farallon plate motion (northeast Eurasia, Alaska and the Aleutians, and Western North America; shown in Fig. 3A and B) is about 15,000 km, which is about 26% of the total length of subduction zones around the world during the Aptian. Assuming that active and passive continental margins store methane hydrates approximately equally, and were approximately equal to each other in length, about 13% of the Aptian methane hydrate reservoir (=1300 Gt C) could be found within the affected subduction zones of the early Aptian Farallon plate. Methane hydrates are typically concentrated within sediment pore space located 500–3000 m below sea level [60]; below 3000 m the amount of methane in most deep-ocean sediments is insufficient for hydrate generation [61]. Given the above, we consider uplift on the order of a few kilometers to be sufficient to destabilize gigatons of methane clathrates during the early Aptian.

We calculated that horizontal shortening of the overriding plate resulting from increased seismic coupling (Fig. 4) uplifted the continental margin of the northern Pacific basin by as much as 4.0 km in 1 Myr (Fig. 3D). Comprehensive geological observations of early Aptian uplift and convergence [43] confirm our predicted pattern of uplift ((Fig. 3D). As discussed above, the position of methane hydrates within continental margins suggests that ~2.5 km of uplift is required to destabilize the entire reservoir of methane hydrates stored along a given continental margin. Our calculation of uplift (Fig. 3D), which assumes a shortening width of W=250 km along the affected convergent zone (=15,000 km of coastline), suggests a total release of methane hydrates=910 Gt C over 1 Myr (Fig. 3D), including the effects of partial uplift. This value is equivalent to ~80% of the methane hydrate release implied by the stable isotope records presented above (1137 Gt of C).

The above estimate of uplift is a conservative one and does not include several other processes that would increase the rate of uplift due to the onset of horizontal shortening. Thus, the amount of methane hydrate release shown in Fig. 3D is also a conservative estimate. There are three main processes that would act to increase uplift relative to what is calculated based on the formulation above. First, the expected detachment of the slab from the subducting plate (Fig. 4B) would suddenly remove the downward pull of the slab on the Earth's surface, resulting in significant surface uplift. Buiter et al. [62] have estimated that detachment of a descending slab results in 2–6 km of surface uplift along the continental margin (values that, if invoked, would double or even triple the values we estimate in Fig. 3D). In example, this process is thought have uplifted the New Hebrides islands at about 1 mm/yr since the development of a gap in the Vanuatu slab during the last 0.5 Myr [63]. Second, when erosion decreases the average height of an uplifted surface, isostatic compensation will raise the exhumed rocks to nearly the original elevation of the surface before erosion [64]. In this way, erosion imparts additional uplift of rocks beyond what was accomplished tectonically. Because erosion rates of a few mm/yr (=km/Ma) are possible for high mountain ranges such as the Andes [65], uplift associated with erosion could be comparable to that of tectonically induced uplift (thus doubling the values in Fig. 3D). Third, if the slab descends more steeply than ~20°, the width of uplift will be reduced. We have already discussed how a ~30° dip yields W=~175 km, which leads to ~40% greater uplift. However, if the width of uplift is reduced to <~200 km, the uplift will also not be completely compensated isostatically. In this case, a larger fraction of crustal thickening may manifest itself as uplift, increasing the rate of uplift (by up to 5×, in the case of no compensation).

All three of these mechanisms, working in concert, should augment tectonic uplift and therefore increase our estimate of methane hydrate release during the early Aptian (Fig. 3D). The amount of additional hydrate release, however, is not proportional to the amount of additional uplift. This is because our conservative model for uplift already produces enough

uplift along some margins (e.g., >2.5 km) to destabilize the entire methane hydrate reservoir (Fig. 3D). For example, a narrower shortening width of $W=175$ km would cause ~40% more uplift but would release only ~17% more methane hydrates (1066 Gt C total). Thus, even if the above uncertainties increase the amount of uplift dramatically, the amount of methane hydrate release cannot significantly exceed our isotopically observed value of 1137 Gt C, because only ~1300 Gt C were likely stored as methane hydrates along the uplifted margin. Thus, we surmise that uplift associated with the locking of the Farallon plate's northern subduction zones likely destabilized a volume of methane hydrates directly comparable to that required by the isotopic measurements (Fig. 2).

7. Conclusion

The early Aptian uplift we suggest likely comprised a series of spasmodic uplift events: increased mechanical coupling is associated with the release of great thrust earthquakes [49,51] and submarine landslides within continental margin sediments. Because of the catastrophic nature of methane hydrate destabilization mechanics, the release of methane hydrates via the deformation of continental margins likely occurred as many rapid bursts during the early Aptian, reflected in the terrestrial and marine $\delta^{13}C$ records (Fig. 2B). Furthermore, conditions favorable for the formation of methane hydrates would be present along the continental margin between episodes of catastrophic destabilization, allowing methane hydrates to accumulate during periods of relative stability and then become periodically re-released once the disruption of the continental margin resumed. This explains the alternating periods of release and sequestration of carbon with $\delta^{13}C=-60‰$ during the early Aptian reflected in Fig. 2B; it also argues for spatial, as well as temporal, variability in methane release along the continental margin of the Pacific basin, as shown by Fig. 3D.

A passive-margin volcanic mechanism has been recently suggested for the methane hydrate release at the PETM [66], additionally highlighting the important role of plate-margin processes in methane hydrate destabilization. These authors [66] discussed the preclusion of a firm temporal correlation between volcanic and isotopic events due to the disparate nature of how each process is recorded in the geologic record; similar caveats apply here. Given the temporal records of all phenomena involved, it is clear that observed early Aptian isotope excursions did not precede the changes in subduction resulting from changing Farallon plate motion. Overall, it is the abrupt sediment deformation associated with changes in subduction, in addition to comparable carbon releases implied by both the tectonic and the isotopic records, that comprises the strongest argument for control of methane hydrate release by dramatic tectonic events. Our results for the Aptian have the potential to link plate tectonics to the Earth's climate system via methane release, and propose a mechanism that is capable of engaging sporadically, and independently, from other carbon cycle processes.

Acknowledgements

This work was funded by NSF-EAR 0106171 and the David and Lucille Packard Foundation. We thank J.A. Doyle, D.G. De Paor, U. Heimhofer, J.P. Montoya and two anonymous reviewers for input and comments; we thank W.M. Hagopian for laboratory analysis and C.J. Conrad for inspiring this particular collaboration.

Appendix A. Materials and methods

The Arundel Clay Formation of the Potomac Group was sampled within the United Clay Mine, NE of White Marsh, Baltimore County, Maryland. These organic-rich terrestrial mudstones and lignitic clays have yielded key information about Early Cretaceous ecosystems: the pollen fossilized within the Arundel Formation reflects the initial diversification and geographic expansion of flowering plants [67]; the Arundel also contains the only vertebrate (dinosaur and mammal) fossils of Early Cretaceous age in eastern North America [68]. Eleven meters of exposed section were sampled at 5–10 cm increments in order to capture variations in lamination and organic matter content, resulting in the collection of ~190 samples. Sampling ceased 2 m below the surface in order to exclude sediments altered by Holocene pedogenesis. Bulk organic samples were dried, ground and acidi-

fied in 1 M HCl for 72 h. Plant cuticle was isolated from rock sub-samples by exposure to 60% HF for 1 week, followed by identification and manual separation under the optical microscope at 5× magnification; cuticle morphology was then verified under 40× magnification. Twenty to forty cuticle fragments of mixed taxonomic origin constituted the amount of material necessary for C-isotope determination, which was performed in duplicate and triplicate when sufficient material could be isolated. All samples were analyzed for $^{13}C/^{12}C$ using a Eurovector automated combustion system in conjunction with an Isoprime SIRMS at Johns Hopkins University; combustion also resulted in a quantification of %C in each sample (all values ±1% C analytical uncertainty). Precision associated with the mass spectrometer was within ±0.1‰ in all cases. When triplicate analyses of bulk organic samples yielded a standard deviation ≥2.0‰ the sample was excluded from further interpretation due to the apparent inhomogeneity of the substrate; these inhomogeneous samples also exhibited conspicuously low %C value. Isotopic values are reported according to convention: $\delta=(R_{sample}-R_{standard}/R_{standard})\times 1000$ [‰], $R=^{13}C/^{12}C$ and relative to the Vienna Peedee belemnite standard (VPDB).

Pollen and spores from three widely spaced samples were used to assign stratigraphic age dates to the section. All three samples contained similar palynofloras and were indistinguishable as to age. Fern spores including *Cyathidites minor*, *Gleicheniidites* sp. and *Laevigatosporites gracilis* dominated the samples, taken in conjunction with the samples' very low frequency of tricolpate angiosperm pollen (<1%), our observations correspond to Brenner's [69] assignment of the Arundel Formation to palynological Zone I (Barremian to Aptian in age). Additionally, *C. hughessi* was present but rare in our samples; the presence of *Arcellites disciformis* megaspores further corroborate a Barremian to Aptian age as specified by Batten et al. [70]. Based on angiosperm pollen, Doyle and Robbins [67] tentatively preferred a middle to late Aptian age for the Arundel Formation. We observed rare inclusions of non-columellar *Brenneripollis peroreticulatus* which is Aptian in age [12] and precludes a Barremian assignment for this locality. Furthermore, the grains reported at the United Clay Mine fall into the smaller size class reported from Egypt by Penny [71] who described a distinct size increase at the transition from middle to late Aptian. This suggests that the United Clay Mine section is best aged early to middle Aptian, in keeping with recent vertebrate paleontology of the Arundel Formation [68]. The presence of *Arcellites* (a megaspore likely produced by a water fern of the Marciliaceae) throughout the section suggests that the Arundel Clay was deposited in the quiet, standing freshwater of a pond or lake [70]; an exclusively terrestrial environment is confirmed by the congruence of bulk organic and cuticle isolate $\delta^{13}C_{org}$ values in Arundel Clay samples (Fig. 1 and [72]).

References

[1] G.R. Dickens, Rethinking the global carbon cycle with a large, dynamic and microbially mediated gas hydrate capacitor, Earth Planet. Sci. Lett. 213 (2003) 169–183.

[2] G.R. Dickens, J.R. O'Neil, D.K. Rea, R.M. Owen, Dissociation of oceanic methane hydrate as a cause of the carbon isotope excursion at the end of the Palaeocene, Paleoceanography 10 (1995) 965–971.

[3] E.S. Krull, G.J. Retallack, $\delta^{13}C$ depth profiles from paleosols across the Permian–Triassic boundary: evidence for methane release, Geol. Soc. Amer. Bull. 112 (9) (2000) 1459–1472.

[4] S.P. Hesselbo, D.R. Gröcke, H.C. Jenkyns, C.J. Bjerrum, P. Farrimond, H.S. Morgans-Bell, O.R. Green, Massive dissociation of gas hydrate during a Jurassic oceanic anoxic event, Nature 406 (6794) (2000) 392–395.

[5] H. Padden, H. Weissert, M. DeRafelis, Evidence for Late Jurassic release of methane from gas hydrate, Geology 29 (2001) 223–226.

[6] A.H. Jahren, N.C. Arens, G. Sarmiento, J. Guerrero, R. Amundson, Terrestrial record of methane hydrate dissociation in the Early Cretaceous, Geology 29 (2) (2001) 159–162.

[7] G. Jiang, M.J. Kennedy, N. Christie-Blick, Stable isotope evidence for methane seeps in Neoproterozoic postglacial cap carbonates, Nature 426 (2003) 822–826.

[8] J.C. Zachos, K.C. Lohmann, J.C.G. Walker, S.W. Wise, Abrupt climate change and transient climates during the Palaeogene: a marine perspective, J. Geol. 101 (1993) 191–213.

[9] D.R. Gröcke, S.P. Hesselbo, H.C. Jenkyns, Carbon-isotope composition of Lower Cretaceous fossil wood: ocean–atmosphere chemistry and relation to sea-level change, Geology 27 (2) (1999) 155–158.

[10] A. Ando, T. Kakegawa, R. Takashima, T. Saito, New perspectives on Aptian carbon isotope stratigraphy: data from $\delta^{13}C$ records of terrestrial organic matter, Geology 30 (3) (2002) 227–230.

[11] U. Heimhofer, P.A. Hochuli, S. Burla, N. Anderson, H. Weissert, Terrestrial carbon-isotope records from coastal deposits (Algarve, Portugal): a tool for chemostratigraphic correlation on an intrabasinal and global scale, Terra Nova 15 (2003) 8–13.

[12] J.A. Doyle, Revised palynological correlations of the lower Potomac Group (USA) and the Cocobeach sequence of Gabon (Barremian–Aptian), Cretac. Res. 13 (1992) 337–349.
[13] A. Menegatti, H. Weissert, R.S. Brown, R.V. Tyson, P. Farrimond, A. Strasser, M. Caron, High-resolution $\delta^{13}C$ stratigraphy through the early Aptian "Livello Selli" of the Alpine Tethys, Paleoceanography 13 (1998) 530–545.
[14] N.J. Butterfield, Organic preservation of non-mineralizing organisms and the taphonomy of the Burgess Shale, Paleobiology 16 (1990) 272–286.
[15] D.J. Beerling, M.R. Lomas, D.R. Gröcke, On the nature of methane gas-hydrate dissociation during the Toarcian and Aptian oceanic anoxic events, Am. J. Sci. 302 (2002) 28–49.
[16] N.C. Arens, A.H. Jahren, R. Amundson, Can C3 plants faithfully record the carbon isotopic composition of atmospheric carbon dioxide? Paleobiology 26 (2000) 137–164.
[17] J. Lloyd, G.D. Farquhar, ^{13}C discrimination during CO_2 assimilation by the terrestrial biosphere, Oecologia 99 (1994) 201–215.
[18] R.A. Berner, Z. Kothavala, GEOCARB III; a revised model of atmospheric CO_2 over Phanerozoic time, Am. J. Sci. 301 (2) (2001) 182–204.
[19] B.E. Taylor, Magmatic volatiles: isotopic variation of C, H, and S, Rev. Miner. 16 (1986) 185–231.
[20] T.H. Peng, W.S. Broecker, H.D. Freyer, S. Trumbore, A deconvolution of the tree-ring based $\delta^{13}C$ record, J. Geophys. Res. 88 (C6) (1983) 3609–3620.
[21] K.A. Kvenvolden, Gas hydrates: geological perspectives and global change, Rev. Geophys. 31 (1993) 173–187.
[22] M.L.G. Tejada, J.J. Mahoney, R.A. Duncan, M.P. Hawkins, Age and geochemistry of basement and alkalic rocks of Malaita and Santa Isabel, Solomon Islands, southern margin of Ontong Java Plateau, J. Petrol. 37 (2) (1996) 361–394.
[23] E.T. Sundquist, The global carbon budget, Geology 259 (1993) 934–941.
[24] R. Lupia, S. Lidgard, P.R. Crane, Comparing palynological abundance and diversity; implications for biotic replacement during the Cretaceous angiosperm radiation, Paleobiology 25 (1999) 305–340.
[25] K.A. Kvenvolden, Methane hydrate—a major reservoir of carbon in the shallow geosphere? Chem. Geol. 71 (1988) 41–51.
[26] R.A. Berner, Atmospheric carbon dioxide levels over Phanerozoic time, Science 249 (1990) 1382–1386.
[27] P.D. Deines, D. Langmuir, R.S. Harmon, Stable carbon isotope ratios and the existence of a gas phase in the evolution of carbonate groundwater, Geochim. Cosmochim. Acta 38 (1974) 1147–1164.
[28] J. Zhang, P.D. Quay, D.O. Wilbur, Carbon isotope fractionation during gas–water exchange and dissolution of CO_2, Geochim. Cosmochim. Acta 59 (1) (1995) 107–114.
[29] E.T. Sundquist, Geological perspective on CO_2 and the C cycle, in: E.T. Sundquist, W.S. Broecker (Eds.), The Carbon Cycle and Atmospheric CO_2: Natural Variations Archaean to Present, AGU Press, 1985, pp. 5–59.
[30] J.W. Morse, F.T. Mackenzie, Hadean ocean carbonate geochemistry, Aquat. Geochem. 4 (1998) 301–319.
[31] C.L. Sabine, R.A. Feely, N. Gruber, R.M. Key, K. Lee, J.L. Bullister, R. Wanninkhof, C.S. Wong, D.W.R. Wallace, B. Tilbrook, F.J. Millero, T.H. Peng, A. Kozyr, T. Ono, A.F. Rios, The oceanic sink for anthropogenic CO_2, Science 305 (2004) 367–371.
[32] F. Joos, M. Bruno, Long-term variability of the terrestrial and oceanic carbon sinks and the budgets of the carbon isotopes ^{13}C and ^{14}C, Global Biogeochem. Cycles 12 (2) (1998) 277–295.
[33] Y. Zhang, Methane escape from gas hydrate systems in the marine environment, and methane-driven oceanic eruptions, Geophys. Res. Lett. 30 (2003), doi:10.1029/2002GL016658.
[34] U. Siegenthaler, J.L. Sarmiento, Atmospheric carbon dioxide and the ocean, Nature 365 (1993) 119–125.
[35] J.F. Barker, P. Fritz, Carbon isotope fractionation during microbial methane oxidation, Nature 293 (5830) (1981) 289–291.
[36] A.K. Snover, P.D. Quay, Hydrogen and carbon kinetic isotope effects during soil uptake of atmospheric methane, Global Biogeochem. Cycles 14 (1) (2000) 25–39.
[37] G. Saueressig, J.N. Crowley, P. Bergamaschi, C. Brühl, C.A.M. Brenninkmeijer, H. Fischer, Carbon 13 and D kinetic isotope effects in the reactions of CH_4 with $O(^1D)$ and OH: new laboratory measurements and their implications for the isotopic composition of stratospheric methane, J. Geophys. Res. 106 (D19) (2001) 23127–23138.
[38] J. Lelieveld, P.J. Crutzen, F.J. Dentener, Changing concentration, lifetime and climate forcing of atmospheric methane, Tellus 50B (1998) 128–150.
[39] M.J. Prather, Time scales in atmospheric chemistry: theory, GWPs for CH_4 and CO, and runaway growth, Geophys. Res. Lett. 23 (19) (1996) 2597–2600.
[40] W.S. Borowski, A review of methane and gas hydrates in the dynamic, stratified system of the Blake Ridge region, offshore southeastern North America, Chem. Geol. 205 (3–4) (2004) 311–346.
[41] R.L. Larson, Latest pulse of Earth: evidence for a mid-Cretaceous superplume, Geology 19 (1991) 547–550.
[42] A.H. Jahren, The biogeochemical consequences of the mid-Cretaceous superplume, J. Geodyn. 34 (2) (2002) 177–191.
[43] A.P.M. Vaughan, Circum-Pacific mid-Cretaceous deformation and uplift: a superplume-related event? Geology 23 (6) (1995) 491–494.
[44] P.L. Heller, D.L. Anderson, C.L. Angevine, Is the middle Cretaceous pulse of tapid sea-floor spreading real or necessary? Geology 24 (1996) 491–494.
[45] J. Hardebeck, D.L. Anderson, Eustasy as a test of a Cretaceous superplume hypothesis, Earth Planet. Sci. Lett. 137 (1996) 101–108.
[46] D.C. Engebretson, A. Cox, R.G. Gordon, Relative motions between oceanic and continental plates in the Pacific basin, Spec. Pap.-Geol. Soc. Am. 206 (1985) 1–59.
[47] C. Lithgow-Bertelloni, M.A. Richards, The dynamics of Cenozoic and Mesozoic plate motions, Rev. Geophys. 36 (1998) 27–78.

[48] D.C. Engebretson, A. Cox, R.G. Gordon, Relative motions between oceanic plates of the Pacific basin, J. Geophys. Res. 89 (1984) 10291–10310.
[49] C.P. Conrad, S. Bilek, C. Lithgow-Bertelloni, Great earthquakes and slab pull: interaction between seismic coupling and plate–slab coupling, Earth Planet. Sci. Lett. 218 (2004) 109–122.
[50] C.M. Rubin, E.L. Miller, J. Toro, Deformation of the northern circum-Pacific margin: variations in tectonic style and plate-tectonic implications, Geology 23 (1995) 897–900.
[51] S. Uyeda, H. Kanamori, Back-arc opening and the mode of subduction, J. Geophys. Res. 84 (1979) 1049–1061.
[52] L. Ruff, H. Kanamori, Seismicity and the subduction process, Phys. Earth Planet. Inter. 23 (1980) 240–252.
[53] W.D. Mooney, G. Laske, T.G. Masters, CRUST 5.1: a global crustal model at 5 degrees by 5 degrees, J. Geophys. Res. 103 (1998) 727–747.
[54] R.D. Jarrard, Relations among subduction parameters, Rev. Geophys. 24 (1986) 217–284.
[55] G.R. Dickens, M.S. Quinby-Hunt, Methane hydrate stability in pore water: a simple theoretical approach for geophysical applications, J. Geophys. Res. 102 (B1) (1997) 773–783.
[56] P.R. Miles, Potential distribution of methane hydrate beneath the European continental margins, Geophys. Res. Lett. 22 (23) (1995) 3179–3182.
[57] B.A. Buffet, Clathrate hydrates, Ann. Rev. Earth Planet. Sci. 28 (2000) 477–507.
[58] G.R. Dickens, The potential volume of oceanic methane hydrates with variable external conditions, Org. Geochem. 32 (10) (2001) 1179–1193.
[59] B. Buffett, D. Archer, Global inventory of methane clathrate: sensitivity to changes in the deep ocean, Earth Planet. Sci. Lett. 227 (2004) 185–199.
[60] J.F. Bratton, Clathrate eustasy: methane hydrate melting as a mechanism for geologically rapid sea-level fall, Geology 27 (10) (1999) 915–918.
[61] V. Gornitz, I. Fung, Potential distribution of methane hydrate in the world's oceans, Global Biogeochem. Cycles 8 (1994) 335–347.
[62] S.J.H. Buiter, R. Govers, M.J.R. Wortel, Two-dimensional simulations of surface deformation caused by slab detachment, Tectonophysics 354 (2002) 195–210.
[63] J.-L. Chatelain, P. Molnar, R. Prevot, B. Isacks, Detachment of part of the downgoing slab and uplift of the New Hebrides (Vanuatu) islands, Geophys. Res. Lett. 19 (1992) 1507–1510.
[64] P. Molnar, P. England, Late Cenozoic uplift of mountain ranges and global climate change: chicken or egg? Nature 346 (1990) 29–34.
[65] D.R. Montgomery, G. Balco, S.D. Willett, Climate, tectonics, and the morphology of the Andes, Geology 29 (2001) 579–582.
[66] H. Svensen, S. Planke, A. Malthe-Søenssen, B. Jamtvelt, R. Myklebust, T.R. Eldem, S.R. Rey, Release of methane from a volcanic basin as a mechanism for initial Eocene global warming, Nature 429 (2004) 542–545.
[67] J.A. Doyle, E.I. Robbins, Angiosperm pollen zonation of the continental Cretaceous of the Atlantic Coastal Plain and its application to deep wells in the Salisbury embayment, in: R.L. Pierce (Ed.), Proceedings of the Eighth Annual Meeting of the American Association of Stratigraphic Palynologists, 1977, pp. 43–78.
[68] K.D. Rose, R.L. Cifelli, T.R. Lipka, Second Triconodont dentary from the Early Cretaceous of Maryland, J. Vertebr. Paleontol. 21 (3) (2001) 628–632.
[69] G.J. Brenner, The spores and pollen of the Potomac Group of Maryland, Maryland, Dept. Geol. Mines, Water Resour. Bull. 27 (1963) 215.
[70] D.J. Batten, R.J. Butta, E. Knobloch, Differentiation, affinities and palaeoenvironmental significance of the megaspores Arcellites and Bohemisporites in Welden and other Cretaceous successions, Cretac. Res. 17 (1996) 39–65.
[71] J.H. Penny, Early Cretaceous acolumellate semitectate pollen from Egypt, Palaeontology 31 (1988) 373–418.
[72] N.C. Arens, A.H. Jahren, Chemostratigraphic correlation of four fossil-bearing sections in southwestern North Dakota, in: J.H. Hartman, K.R. Johnson, D.J. Nichols (Eds.), The Hell Creek Formation and the Cretaceous–Tertiary Boundary in the Northern Great Plains: An Integrated Record of the End of the Cretaceous, vol. 361, Geological Society of America Special Paper, Boulder, Colorado, 2002, pp. 75–93.